A Journal of the Gesellschaft Deutscher Chemiker

Angewandte International Edition GDCh Chemie

www.angewandte.org

Accepted Article

Title: Oxygen evolution electrocatalysis of a single MOF-derived composite nanoparticle on the tip of a nanoelectrode

Authors: Harshitha Barike Aiyappa, Patrick Wilde, Thomas Quast, Justus Masa, Corina Andronescu, Yen-Ting Chen, Martin Muhler, Roland A. Fischer, and Wolfgang Schuhmann

To be cited as: *Angew. Chem. Int. Ed.* 10.1002/anie.201903283
Angew. Chem. 10.1002/ange.201903283

Link to VoR: http://dx.doi.org/10.1002/anie.201903283
http://dx.doi.org/10.1002/ange.201903283

WILEY-VCH

10.1002/anie.201903283

WILEY-VCH

COMMUNICATION

Oxygen evolution electrocatalysis of a single MOF-derived composite nanoparticle on the tip of a nanoelectrode

Harshitha Barike Aiyappa [a], Patrick Wilde [a], Thomas Quast [a], Justus Masa [a], Corina Andronescu [b], Yen-Ting Chen [a], Martin Muhler [c], Roland A. Fischer [d], Wolfgang Schuhmann [a]*

Abstract: Determination of the intrinsic electrocatalytic activity of nanomaterials by means of macroelectrode techniques is compromised by ensemble and film effects. Here, a unique 'particle at the stick' approach is used to grow a single metal-organic framework (MOF; ZIF-67) nanoparticle on a nanoelectrode surface which is pyrolyzed to generate a cobalt/nitrogen-doped carbon (CoN/C) composite nanoparticle that exhibits very high catalytic activity towards the oxygen evolution reaction (OER) with a current density of up to 230 mA cm^{-2} at 1.77 V (vs. RHE), and a high turn-over frequency (TOF) of 29.7 s^{-1} at 540 mV overpotential. Identical location transmission electron microscopy (IL-TEM) analysis substantiates the 'self-sacrificial' template nature of the MOF, while post-electrocatalysis studies reveal agglomeration of Co centers within the Co-N/C composite during the OER. 'Single-entity' electrochemical analysis allows for deriving the intrinsic electrocatalytic activity apart from furnishing insights into the transient behavior of the electrocatalyst under reaction conditions.

'Single-entity electrochemistry' aims to understand electrochemical phenomena at the molecular level down to individual electroactive sites, to ultimately explain fundamentals of electrochemical reactions.[1] This concept gained momentum after ultra-small electrodes became accessible, which are capable of identifying transient, highly sensitive, ultra-low amplitude signals resulting from the electrochemical response of nanoscale entities.[2] Its inception marks a new frontier in 'single-entity' studies, breaking away from deducing nanoparticle behavior from bulk-continuum statistical ensemble analysis at macroelectrodes.[3] The nanometric dimensions of the electrode support investigations of reaction kinetics at much higher mass transport rates owing to hemispherical diffusion towards the electrode along with negligible charging currents and low effects of uncompensated solution resistance.[4] They also allow monitoring kinetics of very fast electrochemical events in small volumes and unusual electrolytes.[5] The enhanced mass transport rate allows circumvention of ensemble and film effects, which are usually encountered while analyzing electrode reactions macroscopically.

[a] Dr. H. B. Aiyappa, P. Wilde, T. Quast, Dr. J. Masa, Dr. Y.-T. Chen, Prof. Dr. W. Schuhmann
Analytical Chemistry – Center for Electrochemical Sciences (CES); Faculty for Chemistry and Biochemistry; Ruhr University Bochum; D-44780 Bochum, Germany
wolfgang.schuhmann@rub.de
[b] Prof. Dr. C. Andronescu
Chemical Technology III, Faculty of Chemistry and CENIDE, Center for Nanointegration University Duisburg Essen, Carl-Benz-Str. 199; D-47057 Duisburg, Germany
[c] Prof. Dr. M. Muhler
Industrial Chemistry, Faculty of Chemistry and Biochemistry, Ruhr-Universität Bochum; D-44780 Bochum, Germany
[d] Prof. Dr. R. A. Fischer
Department of Chemistry and Catalysis Research Centre, Technical University of Munich, 85748 Garching, Germany

Supporting information for this article is given via a link at the end of the document.

Specifically, a nanoelectrode can provide a platform to combat fluctuations in the local chemical environment proximal to the nanoparticle. For instance, local changes in the interfacial pH value are known to influence molecular transport and the kinetics of electrochemical reactions such as e.g. the OER, the CO_2 reduction reaction, the hydrogen oxidation reaction and the hydrogen evolution reaction.[6] In order to evaluate the intrinsic activity of a given catalyst towards such pH-sensitive reactions, a single catalyst nanoparticle attached to a nanoelectrode should be employed to investigate electron transfer kinetics and the electrocatalytic response. The presence of a single nanoparticle on the nanoelectrode enables the closest approximation of its fundamental properties along with its shape and size-dependent electrocatalytic activity.[7] In particular, it supports binder-free investigation of catalytic activity devoid of any film effects, resistive charge-transfer pathways and 'dead volume' spaces due to additives.[8] Nanoscale electrocatalysis therefore offers a new horizon to connect real-world macroscopic catalyst assemblies and the specific response of a single nanoparticle for designing catalyst materials with high selectivity and specificity to desired reaction pathways.[9] Carbon nanoelectrodes (CNE) are widely employed for local electrochemical measurements.[10] The tunable surface properties of CNEs makes them convenient in cases where a defined chemical surface is needed to promote the growth or attachment of a specific nanoparticle. [11] The ability to tune the size of the CNE to match that of the nanoparticle enables the extraction of important reaction parameters.[12]

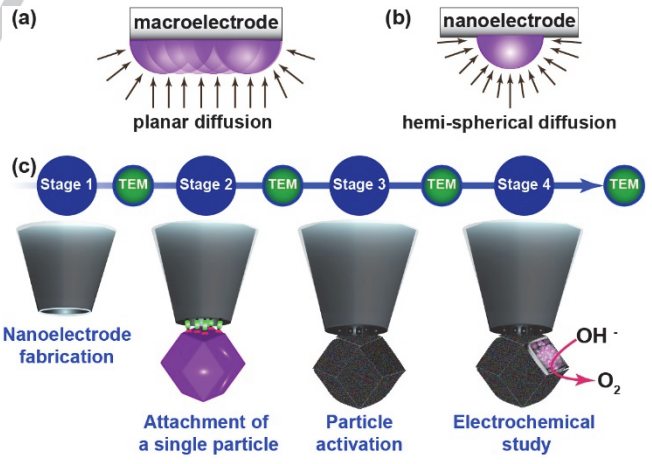

Scheme 1. (a) Illustration of diffusion flux around a macroelectrode and (b) a nanoelectrode. (c) Flowchart of the various stages involved in the MOF-derived CoN/C nanoparticle study.

Several studies exist in which single metal/metal oxide nanoparticles supported on CNE were tested for their voltammetric behavior.[13] A comprehensive understanding of a particle's catalytic activity requires characterization of the structure and compositional changes: (i) as a catalyst precursor and during metamorphosis

10.1002/anie.201903283

to the active catalyst during reaction, (ii) in the activated state, and (iii) after switching off the reaction.[14] However, visualization of the nanoparticle's growth, the subtle transformations occurring in tandem with the electrocatalytic response and the post-electrocatalysis changes in the aftermath of the reaction remain elusive to 'single-entity' studies owing to the difficulty in handling single nanoparticles. To facilitate identical location microscopic analyses coupled with electrochemical studies, a stable nano-assembly that can withstand the stresses exerted under electrocatalytic reaction conditions is important. The present work illustrates the fabrication of a single MOF nanocrystal of a zeolitic imidazolate framework (ZIF) at the tip of a CNE and its transformation through pyrolysis from an electrochemically inactive, but chemically well-defined MOF nanocrystal into a nano-composite of Co^0/CoO_x embedded in nitrogen-doped graphitic carbon (CoN/C; Scheme 1). The cobalt-based ZIF-67 was specifically chosen due to its advantages: (i) it self-assembles at ambient conditions; (ii) it has the ability to nucleate on modified carbon surfaces; (iii) it can be used as a porous 'sacrificial' template for deriving a cobalt and nitrogen co-doped carbon composite with high structural stability and electrocatalytic activity [15]; (iv) it has a molecular well-defined crystal structure [16] which allows for semi-quantitative analysis of the intrinsic electrocatalytic activity of the resulting CoN/C nanocomposite particle.

The synthesis protocol of the ZIF-67 nanocrystals was adapted, following (see Supplementary Section 1).[17] Comparison of the powder X-ray diffraction (PXRD) spectra with a simulated XRD pattern of the sodalite-type ZIF-67 crystal structure confirms the structural identity and phase purity of the as-synthesized ZIF-67 nanocrystals (Fig. S1). The carbon nanoelectrodes (CNE) were fabricated using an automated pyrolysis set-up (Fig. S2),[18] by pyrolytic decomposition of a butane/propane mixture inside pulled quartz capillaries. Scanning electron microscopy (SEM) indicate that the orifice of the as-prepared nanoelectrodes ranges between 250 and 270 nm in diameter (Fig. S3). The tip of the CNE was further trimmed using a focused ion beam (FIB) to expose a solid carbon disk, as envisaged for the ZIF nuclei attachment and growth (Fig. S4). This additional treatment allows uniform tuning of the diameter of the CNE orifice to 500 to 600 nm, which was found to be optimal for the growth and attachment of ZIF-67 nanoparticles (Supplementary Section 2.2). Initial experiments performed using FIB-trimmed CNEs indicate that ZIF-67 nanoparticles prefer to grow on the insulating quartz surface of the CNE rather than on the carbon disk (Fig. S5). The hydrophilicity and surface roughness of the silica layer apparently outcompete the carbon disk in providing nucleation sites for the ZIF-67 nanoparticles. In order to induce nucleation of ZIF-67 on the CNE surface, it was electrografted with terminal carboxylic groups using reductive deposition of the diazonium salt of 4-amino benzoic acid (Fig. 1a).[19] Electroreduction of the diazonium cations at the CNE surface and diazotization were indicated by the reduction wave in the corresponding voltammograms. In all cases, one voltammogram in the potential range from 0 to -0.6 V (*vs.* Ag/AgCl/3 M KCl) at 50 mV s^{-1} sufficed to diazotize the CNE surface (Fig. S6). Disappearance of the reduction wave during the consecutive scan confirmed surface blocking by the first deposited layer.[20] To maximize electrostatic interactions of the carboxylic groups with the Co^{2+} ions from solution, the diazotized CNE (termed f-CNE) was activated by deprotonating the carboxylic groups in a dilute solution of KOH (1 mM). The activated f-CNE was dipped into a methanolic solution containing the ZIF-67 precursors for 8 min, to facilitate the nucleation and growth of a ZIF nanoparticle on the CNE surface (Fig. 1b).

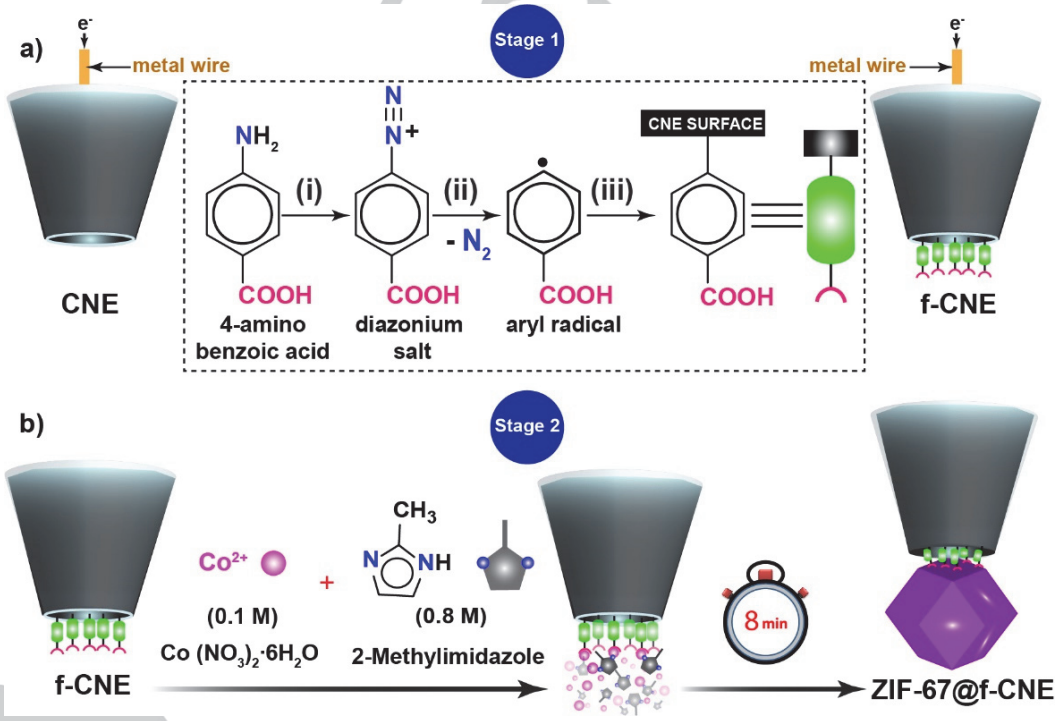

Figure 1. (a) Schematic illustration of the functionalization of a CNE: (i) diazotization of 4-amino benzoic acid; (ii) electroreduction of the diazonium salt; and (iii) electrografting of the carboxylic groups onto the carbon disk. (b) Steps involved in nucleation and subsequent growth of ZIF-67 nanoparticle on f-CNE.

10.1002/anie.201903283

Growth of ZIF-67 nanoparticles on the f-CNE (ZIF-67@f-CNE) was monitored using SEM (Fig. S7b). Importantly, the diazotized CNE only supports the growth and attachment of the ZIF-67 nuclei and does not attach pre-formed ZIF nanoparticles dispersed in solution (Fig. S8).

The f-CNE with attached single ZIF-67 nanoparticle was investigated by means of transmission electron microscopy (TEM) using a specifically designed nanoelectrode holder (Fig. S9). TEM revealed an about 400 nm sized ZIF-67 nanoparticle connected to the carbon disk of the f-CNE (Fig. 2b). Energy-dispersive X-ray spectroscopy (EDX) reveal homogeneous distribution of the ZIF-67 constituting elements throughout the particle (Fig. S10). Elemental TEM-EDX maps differentiate the outer silica cover of the glass sheath from the underlying carbon surface (Fig. 2c). Given the integrity of the electrode architecture throughout the TEM analysis controlled pyrolysis of the attached ZIF-67 nanoparticle was performed. The ZIF-67@f-CNE was pyrolyzed under a counter-flow of argon (99.999 % purity, 50 mL min^{-1} flow rate) at 850 °C using a controlled heating profile (Fig. S11).

The thermally treated ZIF-67@f-CNE (CoN/C@CNE) was re-introduced into the TEM to visualize the changes induced by pyrolysis. TEM images confirmed the intactness of the nano-assembly, with the composite retaining the rhombic dodecahedral morphology of the parent ZIF-67 crystallite (Fig. 2d). EDX maps revealed heterogeneity within the composite, with Co dispersed throughout the graphitic carbon scaffold (Fig. 2e) and nitrogen being uniformly distributed within the carbon matrix (Fig. S12). The nanostructured composite largely comprises of a distorted carbonaceous matrix with Co nanoparticles in the 5 to 30 nm size range embedded inside graphitic carbon domains (Fig. 2f). Lattice fringes with an inter-planar spacing of 0.204 nm correspond to the (111) planes of the metallic Co crystal structure, while lattice fringes with an inter-planar spacing of 0.344 nm correspond to the (002) planes of graphitic carbon.[21] IL-TEM revealed ≈29% volume shrinkage, possibly due to coalescence of Co centres and loss of organic material during pyrolysis (Fig. S13).[22] Preservation of the structural integrity of such a nano-assembly was verified multiple times to ensure reproducibility (Fig. S14).

Retention of the nanoparticle at the CNE tip after pyrolysis is important to allow evaluating single nanoparticle electrocatalysis. The OER activity is remarkably influenced by the local OH^- concentration, interfacial O_2 supersaturation and subsequent shielding of active sites at the catalyst surface by O_2 gas bubbles under macroscopic conditions.[23] One CoN/C@CNE nanoparticle was evaluated for OER electrocatalysis in 0.1 M KOH (Fig. 3c). A thin Cu wire was used to electrically contact the CoN/C@CNE nano-assembly and to evaluate its OER activity in a potential window to up to 1.8 V (*vs.* RHE), at a high scan rate of 200 mV s^{-1} and low electrolyte concentration to avoid or minimize excessive carbon oxidation, which was otherwise observed to erode the composite during slow voltammetric scans in higher concentrated electrolyte (Fig. S15). Upon anodically sweeping the potential at 200 mV s^{-1}, the CoN/C@CNE exhibited low capacitive currents followed by an increase in the catalytic current (Fig. 3e). The OER activity was reproducible during the subsequent voltammetric scans. A blank test using a bare diazotized CNE (diameter 670 nm) without any ZIF-67 modifications (Fig. S16) exhibited negligible catalytic activity (Fig. 3e). Thus, the electrocatalytic activity recorded for CoN/C@CNE can be solely attributed to the catalytic response of the single particle nano-composite.

The nano-assembly's remarkable stability allows investigating the structural properties of the nano-composite particle in the aftermath of electrochemical measurements. The post-electrocatalysis TEM images (Fig. 3f) clearly demonstrate that the composite undergoes drastic restructuring as the Co ions agglomerate within the nano-composite matrix during the OER (Fig. 3g).

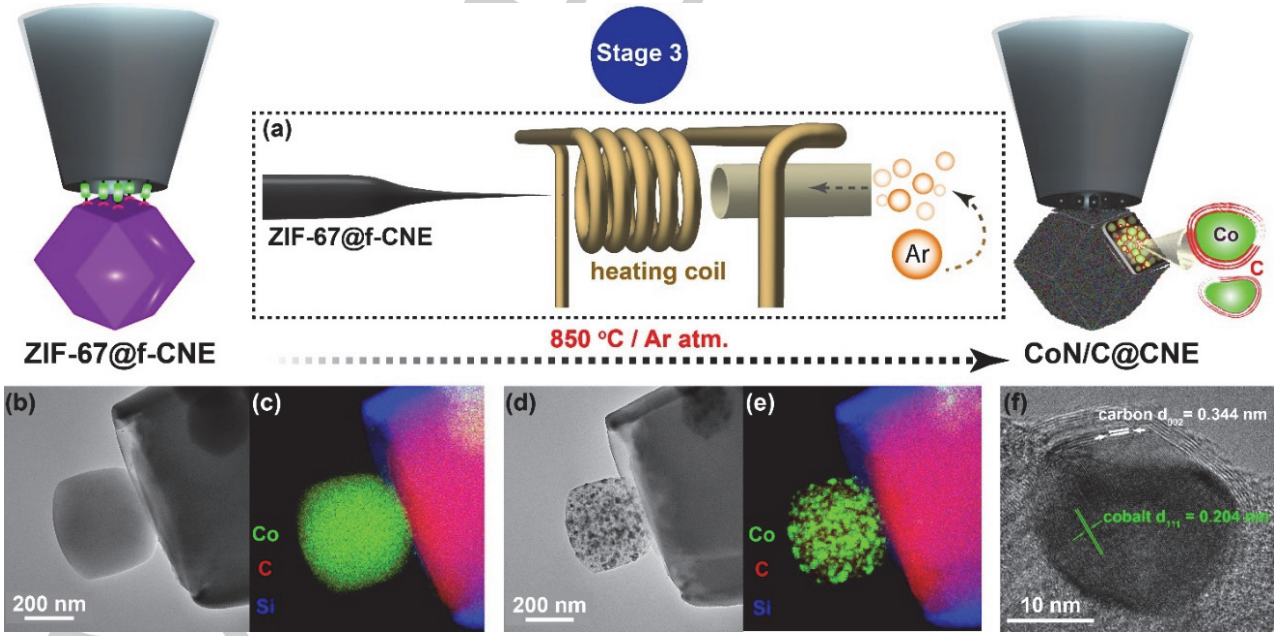

Figure 2. (a) Setup used for pyrolysis of the ZIF-67@f-CNE nano-assembly. (b) TEM image of the ZIF-67@f-CNE nano-assembly and (c) corresponding EDX elemental intensity maps. (d) TEM image of the resulting CoN/C@CNE nano-assembly and (e) corresponding EDX elemental intensity maps. (f) Representative TEM image of a Co-C (core-shell) nanoparticle embedded inside a CoN/C matrix.

10.1002/anie.201903283

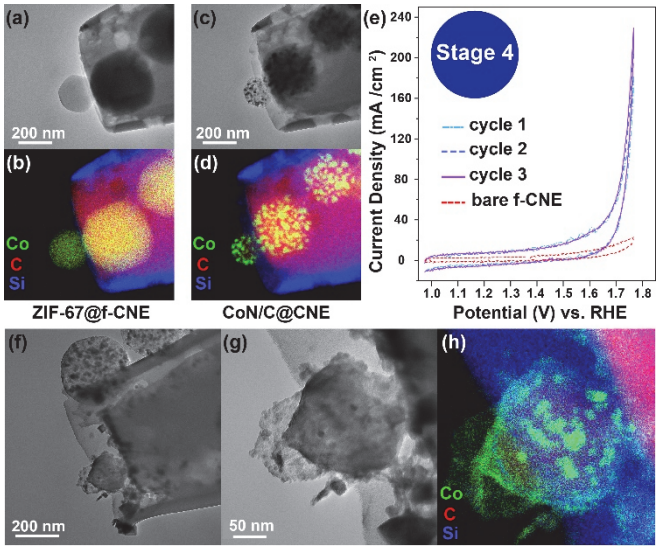

Figure 3. (a) TEM image of the ZIF-67@f-CNE nano-assembly and (b) EDX maps. (c) TEM image of the CoN/C@CNE nano-assembly after pyrolysis and (d) corresponding EDX maps. (e) Cyclic voltammograms recorded using the CoN/C@CNE nano-assembly in 0.1 M KOH at 200 mV s^{-1}. (f) and (g) post-electrocatalysis TEM images of CoN/C@CNE, and (h) corresponding EDX maps.

Importantly, the nearest neighbor composite particles (on the silica surface) remain unaffected by the electrochemical test thereby confirming that these particles did not participate in the electrochemical response (Fig. S17). The presence of electrolyte residues (K^+) throughout the particle suggests an unrestricted diffusion of the electrolyte within the porous matrix during electrocatalysis (Fig. S18). Post-electrocatalysis EDX analysis of the nano-assembly indicates retention of the outer protective quartz sheath (Fig. S19). IL-TEM images of the pyrolyzed composite nanoparticle also validate the 'sacrificial' template nature of ZIF-67 nanocrystals.[24] Estimating the geometric surface area of the nano-composite after considering its mode of attachment on f-CNE (Fig. S20, detailed calculations in Supplementary Section 8), suggests that the nano-composite exhibits extremely high OER rates in 0.1 M KOH, attaining a current density of 230 mA cm^{-2} at 1.77 V (vs. RHE). Measuring such high current density at industrially relevant conditions is practically unattainable using macroelectrodes. Combining the information from the simulated ZIF-67 crystal structure, TEM/STEM images of the CoN/C nano-assembly and the electrochemical study, the amount of Co atoms within the composite matrix is estimated to be 1.66×10^{-17} mol (Fig. S21, detailed calculations in Supplementary Section 9).The turnover frequency (TOF) of the nano-composite particle is calculated based on the assumption that the Co atoms are the active OER sites. At an overpotential of only 0.4 V, the derived TOF for the OER at the 'single-entity' composite particle (4.09 s^{-1}) is almost twice that of monodispersed Co nanoparticles on a carbon surface (2.13 s^{-1}), considering that only the surface Co atoms in the monolayer participate in the OER.[25] A TOF of 4.09 s^{-1} is a conservative estimation, as it assumes that all Co atoms participate in the OER. The MOF-derived nanoparticle exhibits an exceptionally high TOF of 29.7 s^{-1} at an overpotential of 0.54 V, which corroborates the reaction platform provided by the nanoelectrode devoid of contributions from ensemble and film effects. Strikingly, the TOF calculated using TEM/STEM images well agrees with that obtained using the simulated ZIF-67 structure (31.01 s^{-1}). The enhancement in the TOF value highlights the importance of determining the intrinsic activity of an electrocatalyst using such nano-assemblies. Post-electrocatalysis elemental analysis revealed agglomeration of the Co ions within the composite matrix (Fig. 3h). The distinct pattern of cobalt agglomeration inside the composite matrix and the presence of Co residues on the CNE surface suggest that the movement is largely influenced by the hemi-spherical diffusional flux which drives the relocation of the Co ions as they are subjected to oxidation and re-precipitation equilibria as Co hydroxide/oxyhydroxide species.[25,26]

In summary, we report an unprecedented approach toward understanding the electrocatalytic behaviour of single nanoparticles without interference of ensemble and film effects. The scheme of study underpins the potential of such architectures in establishing fundamental electrocatalytic parameters of nanoparticles and structure-property relationships free of macroscopic film effects. Besides the possibility to access fundamental electrocatalytic properties of the nanoparticle, these nano-assemblies can also serve as a powerful platform to study reactions involving variations in the local electrode-electrolyte environment, which is practically inaccessible when using macroelectrodes.

Acknowledgements

This research was funded by the Deutsche Forschungsgemeinschaft (DFG) within the TRR 247 (project number 388390466) EXC-2033 (project number 390677874). H.B.A. acknowledges the Alexander von Humboldt foundation for a postdoc fellowship. P.W. is grateful to the VCI for funding his PhD fellowship. We thank Dr. Sabine Seisel for assistance in PXRD analysis.

Keywords: metal-organic frameworks • electrocatalysis • single nanoparticle • nanoelectrodes • turn-over frequency

[1] L. A. Baker, *J. Am. Chem. Soc.* **2018**, *140*, 15549.
[2] Y.-T. Long, P. R. Unwin, L. A. Baker, *ChemElectroChem* **2018**, *5*, 2918.
[3] J. Clausmeyer, W. Schuhmann, *Trends in Analytical Chemistry* **2016**, *79*, 46.
[4] D. W. M. Arrigan, *Analyst* **2004**, *129*, 1157.
[5] M. A. Edwards, D. A. Robinson, H. Ren, C. G. Cheyne, C. S. Tan, H. S. White, *Faraday Discuss.* **2018**, *210*, 9.
[6] a) J. Ryu, A. Wuttig, Y. Surendranath, *Angew. Chem. Int. Ed.* **2018**, *57*, 9300; b) J. E. Pander, D. Ren, Y. Huang, N. W. X. Loo, S. H. L. Hong, B. S. Yeo, *ChemElectroChem* **2018**, *5*, 219; c) T. Takashima, K. Hashimoto, R. Nakamura, *J. Am. Chem. Soc.* **2012**, *134*, 1519; d) A. Botz, J. Clausmeyer, D. Öhl, T. Tarnev, D. Franzen, T. Turek, W. Schuhmann, *Angew. Chem. Int. Ed.* **2018**, *57*, 12285.
[7] Y. Li, J. T. Cox, B. Zhang, *J. Am. Chem. Soc.* **2010**, *132*, 3047.
[8] P. Wilde, S. Barwe, C. Andronescu, W. Schuhmann, E. Ventosa, *Nano Res.* **2018**, *11*, 6034.
[9] S. E. F. Kleijn, S. C. S. Lai, M. T. M. Koper, P. R. Unwin, *Angew. Chem. Int. Ed.* **2014**, *53*, 3558.
[10] Y. Takahashi, Y. Zhou, T. Fukuma, *Current Opinion in Electrochemistry* **2017**, *5*, 121.

10.1002/anie.201903283

[11] a) R. Zanella, E. V. Basiuk, P. Santiago, V. A. Basiuk, E. Mireles, I. Puente-Lee, J. M. Saniger, *J. Phys. Chem. B* **2005**, *109*, 16290; b) T. Ramanathan, F. T. Fisher, R. S. Ruoff, L. C. Brinson, *Chem. Mater.* **2005**, *17*, 1290; c) Y. Yu, Y. Gao, K. Hu, P.-Y. Blanchard, J.-M. Noël, T. Nareshkumar, K. L. Phani, G. Friedman, Y. Gogotsi, M. V. Mirkin, *ChemElectroChem* **2015**, *2*, 58.

[12] T. Li, W. Hu, *Nanoscale* **2011**, *3*, 166.

[13] a) J. Clausmeyer, A. Botz, D. Öhl, W. Schuhmann, *Faraday Discuss.* **2016**, *193*, 241; b) J. Clausmeyer, J. Masa, E. Ventosa, D. Öhl, W. Schuhmann, *Chem. Commun. (Camb)* **2016**, *52*, 2408; c) V. Brasiliense, J. Clausmeyer, A. L. Dauphin, J.-M. Noël, P. Berto, G. Tessier, W. Schuhmann, F. Kanoufi, *Angew. Chem. Int. Ed.* **2017**, *56*, 10598.

[14] D. S. Su, B. Zhang, R. Schlögl, *Chem. Rev.* **2015**, *115*, 2818.

[15] a) A. Aijaz, J. Masa, C. Rösler, W. Xia, P. Weide, A. J. R. Botz, R. A. Fischer, W. Schuhmann, M. Muhler, *Angew. Chem. Int. Ed.* **2016**, *55*, 4087; b) H. B. Aiyappa, S. N. Bhange, V. P. Sivasankaran, S. Kurungot, *ChemElectroChem* **2017**, *4*, 2928 ; c) J. Tang, Y. Yamauchi, *Nat. Chem.* **2016**, *8*, 638; d) C. Wang, Y. V. Kaneti, Y. Bando, J. Lin, C. Liu, J. Li, Y. Yamauchi, *Mater. Horiz.* **2018**, *5*, 394; e) C. Young, J. Wang, J. Kim, Y. Sugahara, J. Henzie, Y. Yamauchi, *Chem. Mater.* **2018**, *30*, 3379; f) W. Zhang, X. Jiang, Y. Zhao, A. Carné-Sánchez, V. Malgras, J. Kim, J. H. Kim, S. Wang, J. Liu, J.-S. Jiang ,Y. Yamauchi, M. Hu, *Chem. Sci.* **2017**, *8*, 3538.

[16] R. Banerjee, A. Phan, B. Wang, C. Knobler, H. Furukawa, M. O'Keeffe, O. M. Yaghi, *Science* **2008**, *319*, 939.

[17] N. L. Torad, M. Hu, S. Ishihara, H. Sukegawa, A. A. Belik, M. Imura, K. Ariga, Y. Sakka, Y. Yamauchi, *Small* **2014**, *10*, 2096.

[18] P. Wilde, T. Quast, H. B. Aiyappa, Y.-T. Chen, A. Botz, T. Tarnev, M. Marquitan, S. Feldhege, A. Lindner, C. Andronescu et al., *ChemElectroChem* **2018**, *5*, 3083.

[19] D. Bélanger, J. Pinson, *Chem. Soc. Rev.* **2011**, *40*, 3995.

[20] a) A. Laforgue, T. Addou, D. Bélanger, *Langmuir* **2005**, *21*, 6855; b) J. Liu, L. Cheng, B. Liu, S. Dong, *Langmuir* **2000**, *16*, 7471.

[21] a) X. Wang, J. Zhou, H. Fu, W. Li, X. Fan, G. Xin, J. Zheng, X. Li, *J. Mater. Chem. A* **2014**, *2*, 14064; b) W. Zhang, X. Jiang, X. Wang, Y. V. Kaneti, Y. Chen, J. Liu, J.-S. Jiang, Y. Yamauchi, M. Hu, *Angew. Chem. Int. Ed.* **2017**, *56*, 8435.

[22] a) Q. Ma, S. Dutta, K. C.-W. Wu, T. Kimura, *Chem. Eur. J.* **2018**, *24*, 6886; b) H. B. Wu, X. W. D. Lou, *Sci. Adv.* **2017**, *3*, eaap9252.

[23] a) L. Giordano, B. Han, M. Risch, W. T. Hong, R. R. Rao, K. A. Stoerzinger, Y. Shao-Horn, *Catal. Today* **2016**, *262*, 2; b) A. R. Zeradjanin, A. A. Topalov, Q. van Overmeere, S. Cherevko, X. Chen, E. Ventosa, W. Schuhmann, K. J. J. Mayrhofer, *RSC Adv.* **2014**, *4*, 9579.

[24] B. Liu, H. Shioyama, T. Akita, Q. Xu, *J. Am. Chem. Soc.* **2008**, *130*, 5390.

[25] L. Wu, Q. Li, C. H. Wu, H. Zhu, A. Mendoza-Garcia, B. Shen, J. Guo, S. Sun, *J. Am. Chem. Soc.* **2015**, *137*, 7071.

[26] T. Zidki, L. Zhang, V. Shafirovich, S. V. Lymar, *J. Am. Chem. Soc.* **2012**, *134*, 14275.

10.1002/anie.201903283

WILEY-VCH

COMMUNICATION

Electrocatalysis at the tip. A unique 'particle at the stick' approach is employed to extract the intrinsic catalytic activity of a single ZIF-67-derived Co/N-doped carbon nano-composite under industrially relevant OER conditions. Identical location-TEM analyses of the nano-assembly offers insight into structural transformations within the nanoparticle during the pyrolytic activation process and after electrocatalytic activity measurement at extremely high oxygen evolution rates.

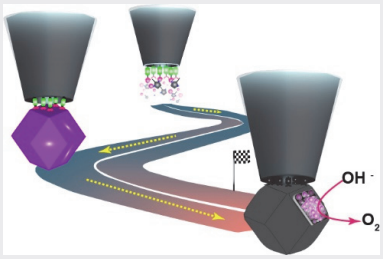

*Harshitha Barike Aiyappa, Patrick Wilde, Thomas Quast, Justus Masa, Corina Andronescu, Yen-Ting Chen, Martin Muhler, Roland A. Fischer, Wolfgang Schuhmann**

Page No. – Page No.

Oxygen evolution electrocatalysis of a single MOF-derived composite nanoparticle on the tip of a nanoelectrode